Article

Possible Mechanism of Proton Transfer through Peptide Groups in the H-Pathway of the Bovine Cytochrome *c* Oxidase

Katsumasa Kamiya, Mauro Boero, Masaru Tateno, Kenji Shiraishi, and Atsushi Oshiyama

J. Am. Chem. Soc., **2007**, 129 (31), 9663-9673• DOI: 10.1021/ja070464y • Publication Date (Web): 18 July 2007

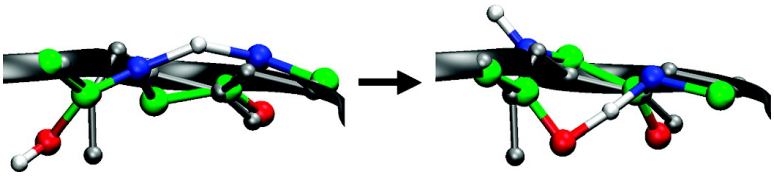

J|A|C|S
ARTICLES
Published on Web 07/18/2007

Possible Mechanism of Proton Transfer through Peptide Groups in the H-Pathway of the Bovine Cytochrome *c* Oxidase

Katsumasa Kamiya,[†,‡] Mauro Boero,*[,†,‡,§] Masaru Tateno,[†,‡,§] Kenji Shiraishi,[‡,§] and Atsushi Oshiyama[†,‡,§]

Contribution from the Center for Computational Sciences, University of Tsukuba, 1-1-1 Tennodai, Tsukuba, 305-8577, Japan, CREST, Japan Science and Technology Agency, 4-1-8 Honcho, Kawaguchi, 332-0012, Japan, and Graduate School of Pure and Applied Sciences, University of Tsukuba, 1-1-1 Tennodai, Tsukuba, 305-8571, Japan

Received January 22, 2007; E-mail: boero@comas.frsc.tsukuba.ac.jp

Abstract: The peptide group connecting Tyr440 and Ser441 of the bovine cytochrome *c* oxidase is involved in a recently proposed proton-transfer path (H-path) where, at variance with other pathways (D- and K-paths), a usual hydrogen-bond network is interrupted, thus making this proton propagation rather unconventional. Our density-functional based molecular dynamics simulations show that, despite this anomaly and provided that a proton can reach a nearby water, a multistep proton-transfer pathway can become a viable pathway for such a reaction: A proton is initially transferred to the carbonyl oxygen of a keto form of the Tyr440-Ser441 peptide group [−CO−NH−], producing an imidic acid [−C(OH)−NH−] as a metastable state; the amide proton of the imidic acid is then transferred, spontaneously to the deprotonated carboxyl group of the Asp51 side chain, leading to the formation of an enol form [−C(OH)═N−] of the Tyr440-Ser441 peptide group. Then a subsequent enol-to-keto tautomerization occurs via a double proton-transfer path realized in the two adjacent Tyr440-Ser441 and Ser441-Asp442 peptide groups. An analysis of this multistep proton-transfer pathway shows that each elementary process occurs through the shortest distance, no permanent conformational changes are induced, thus preserving the X-ray crystal structure, and the reaction path is characterized by a reasonable activation barrier.

1. Introduction

The proton-transfer process in proteins has a wealth of crucial roles in several biological functions such as, for instance, energy transduction. Focusing specifically on cell respiration, it has been understood that in mitochondria the proton transfer through transmembrane proteins, such as the cytochrome *c* oxidase (CcO), is a key step of the general proton pumping function. Namely, protons are pumped from the mitochondrial matrix to the intermembrane space by the inner mitochondrial membrane-bound proteins to create an electrochemical proton gradient, which is eventually harnessed to the synthesis of ATP.[1] Recent researches in bioenergetics have thus focused on the identification of proton-transfer pathways and the elucidation of the mechanisms in such proton-pumping enzymes.[2] In particular, the CcO has been the subject of extensive investigations for proton-transfer mechanisms inside proteins owing to the high-resolution X-ray structure available[3−7] along with its importance in a variety of physiological functions in the metabolism of aerobic cells.

The CcO is the terminal enzyme in the respiratory chain of both mitochondria and aerobic bacteria. Its specific action is to pump protons across the inner mitochondrial membrane or bacterial cytoplasmic membrane, coupled with the O_2 reduction. By an analysis of the crystal structures, two pathways driven by two distinct hydrogen bond (H-bond) networks, called K-pathway and D-pathway, have been proposed both in bacterial and bovine CcO (Figure 1).[5,6] These networks are formed by side chains of amino acid residues and crystallographically ordered water molecules, and both are considered to be active pathways along which protons can be transferred sequentially via a Grotthuss-like proton wire mechanism.[8,9]

Besides the K- and D-pathways, a novel proton-transfer path, named H-pathway, has been proposed for the bovine CcO on the basis of accurate and very high-resolution crystal structures.[3,10,11] Being that these studies are still at a pioneering stage and at the forefront of biology and biochemistry, none of these

† Center for Computational Sciences, University of Tsukuba.
‡ CREST, Japan Science and Technology Agency.
§ Graduate School of Pure and Applied Sciences, University of Tsukuba.

(1) Voet, D.; Voet J. G. *Biochemistry*, 3rd ed.; John Wiley and Sons: Hoboken, NJ, 2004.
(2) Decoursey, T. E. *Physiol. Rev.* **2003**, *83*, 476−579.
(3) (a) Tsukihara, T.; Shimokata, K.; Katayama, Y.; Shimada, H.; Muramoto, K.; Aoyama, H.; Mochizuki, M.; Shinzawa-Itoh, K.; Yamashita, E.; Yao, M.; Ishimura, Y.; Yoshikawa, S. *Proc. Natl. Acad. Sci. U.S.A.* **2003**, *100*, 15304−15309. (b) Brookhaven Protein Data Bank, entry number 1V54.
(4) Ostermeir, C.; Harrenga, A.; Ermler, U.; Michel, H. *Proc. Natl. Acad. Sci. U.S.A.* **1997**, *94*, 10547−10553.
(5) Svensson-Ek, M.; Abramson, J.; Larsson, G.; Törnroth, S.; Brzezinski, P.; Iwata, S. *J. Mol. Biol.* **2002**, *321*, 329−339.
(6) Brzezinski, P.; Larsson, G. *Biochim. Biophys. Acta* **2003**, *1605*, 1−13.
(7) Yoshikawa, S. *Adv. Protein Chem.* **2002**, *60*, 341−395.
(8) Pomés, R.; Roux, B. *J. Phys. Chem.* **1996**, *100*, 2519−2527.
(9) Agmon, N. *Chem. Phys. Lett.* **1995**, *244*, 456−462.

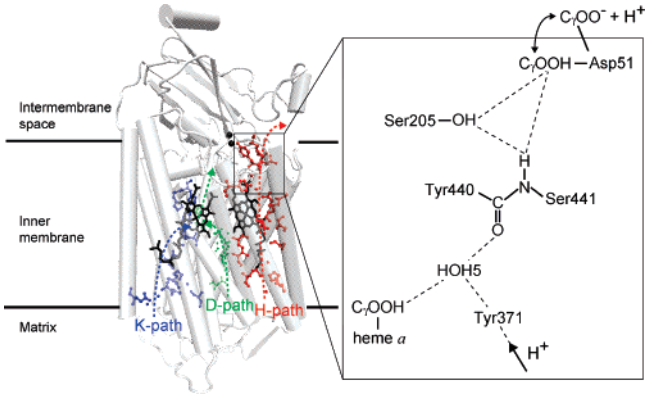

Figure 1. Schematic representation of three proposed proton-transfer paths in the bovine CcO: K-path, D-path, and H-path are shown in blue, green, and red, respectively. Subunits I and II taken from the X-ray structure of the fully oxidized bovine CcO[3] and the redox-active metal sites (shown as either black dots or black sticks) are indicated. The dotted lines in the right panel show the local hydrogen bond network.

proposed pathways has received direct confirmation to date. As far as the specific H-path is concerned, its novelty stems from the presence of a peptide group in the pathway (Figure 1) that interrupts a regular H-bond network, contrary to the other two H-paths mentioned above. Namely, although the major part of the H-path consists of an H-bond network, the peptide group between Tyr440 and Ser441 is on the way and breaks the network into two parts. The first part starts from water cavities located near the matrix side, passes close to the heme *a*, and terminates at a crystal water molecule (HOH5) placed in the vicinity of the carbonyl oxygen of the Tyr440-Ser441 peptide group. On the other hand, the second part comprises Ser205 and Asp51, both located at H-bond distances from the amide nitrogen of the Tyr440-Ser441 peptide group. Upon reduction of the enzyme, the Asp51 residue, which is the final proton acceptor in this path, undergoes a significant movement toward the intermembrane space.

During the past few years, a number of mutagenesis experiments have been performed on several crucial amino acid residues, such as Ser441 and Asp51, present along the H-pathway.[3,12] As far as the Tyr440-Ser441 peptide group is concerned, the mutants in which the peptide group lacks its amide proton because of the replacement of Ser441 with proline (Ser441Pro) do not show any proton pumping activity but just O_2 reduction. These experiments clearly indicate that the Tyr440-Ser441 peptide group is likely to contribute to the proton-transfer process in the bovine CcO. Nonetheless the fundamental proton-transfer mechanism through the Tyr440-Ser441 peptide group in this enzyme is still far from being unraveled.

A detailed atomistic simulation complements the experiments and sheds light on this complex biochemical reaction. In this respect, density functional theory (DFT)[13,14] in combination with

Scheme 1

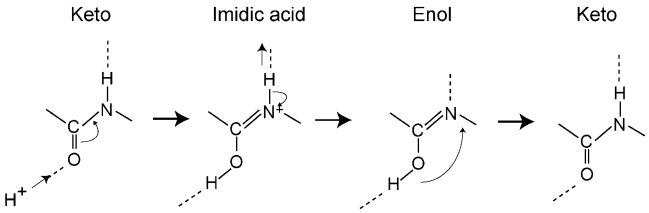

methods suitable to sample reaction paths represents a computationally efficient approach with a variety of successful applications to chemical and biochemical reactions.[15−20] More recently, the metadynamics approach[21,22] combined with Car−Parrinello (CP) molecular dynamics[23] has been shown to be a versatile tool to explore the free-energy surface of a given set of reaction coordinates and allows for a microscopic insight into reaction pathways within affordable simulation times.[24,25]

The purpose of the present work is to use these approaches to elucidate the peculiar proton-transfer mechanism through the Tyr440-Ser441 peptide group in the bovine CcO. As a starting point, we refer to a sequential reaction (Scheme 1) studied experimentally[26] and theoretically[27] in peptide model systems such as *N*-formylglycine and polyglycine. In the reaction, an enol form [−C(OH)═N−] of peptide groups is formed via an imidic acid [−C(OH)−NH−] and subsequently tautomerizes to the keto form [−CO−NH−] as a consequence of the higher stability of the keto with respect to the enol. The difference in the relative stability between the enol and keto forms has been suggested to be responsible for the unidirectionality of proton transfer through the peptide group.[3,7,10,11] To apply this reaction paradigm to the bovine CcO, we focus on the structural features around the Tyr440-Ser441 peptide group in this enzyme (Figure 2). According to the bovine CcO crystal structure,[3] the Try440-Ser441 peptide group forms H-bonds with the crystal water molecule HOH5 and the Asp51 side chain. The scenario that can be drawn is that a proton can reach the carbonyl oxygen of the Tyr440-Ser441 peptide group through the crystal water HOH5, that hence should revert to OH_3^+, by a conventional proton wire mechanism[8,9] (labeled as a in Figure 2), producing the imidic acid of the peptide group; then, the deprotonated carboxyl group ($C_\gamma OO^-$) of the Asp51 side chain promotes the deprotonation of the imidic acid (b in Figure 2), leading to the formation of the enol form.

The subsequent enol-to-keto tautomerization, which is accompanied by a proton transfer through the Tyr440-Ser441

(10) Yoshikawa, S.; Muramoto, K.; Shinzawa-Itoh, K.; Aoyama, H.; Tsukihara, T.; Ogura, T.; Shimokata, K.; Katayama, Y.; Shimada, H. *Biochim. Biophys. Acta* **2006**, *1757*, 395−400.
(11) Yoshikawa, S.; Muramoto, K.; Shinzawa-Itoh, K.; Aoyama, H.; Tsukihara, T.; Shimokata, K.; Katayama, Y.; Shimada, H. *Biochim. Biophys. Acta* **2006**, *1757*, 1110−1116.
(12) Shimokata, K.; Katayama, Y.; Murayama, H.; Muramoto, K.; Suematsu, M.; Tsukihara, T.; Muramoto, K.; Aoyama, H.; Yoshikawa, S.; Shimada. H. *Proc. Nat. Acad. Sci. U.S.A.* **2007**, *104*, 4200−4205.
(13) Hohenberg, P.; Kohn, W. *Phys. Rev.* **1964**, *136*, B864−B871.
(14) Kohn, W.; Sham, L. J. *Phys. Rev.* **1965**, *140*, A1133−A1138.
(15) Barone, V.; Adamo, C. *J. Chem. Phys.* **1996**, *105*, 11007−11019.
(16) Sadhukhan, S.; Muñoz, D.; Adamo, C.; Scuseria, G. E. *Chem. Phys. Lett.* **1999**, *306*, 83−87.
(17) Aplincourt, P.; Bureau, C.; Anthoine, J-L.; Chong, D. P. *J. Phys. Chem. A* **2001**, *105*, 7364−7370.
(18) Boero, M.; Terakura, K.; Tateno, M. *J. Am. Chem. Soc.* **2002**, *124*, 8949−8957.
(19) Boero, M.; Ikeshoji, T.; Liew, C. C.; Terakura, K.; Parrinello, M. *J. Am. Chem. Soc.* **2004**, *126*, 6280−6286.
(20) Boero, M.; Tateno, M.; Terakura, K.; Oshiyama, A. *J. Chem. Theory Comput.* **2005**, *1*, 925−934.
(21) Iannuzzi, M.; Laio, A.; Parrinello, M. *Phys. Rev. Lett.* **2003**, *90*, 238302.
(22) Laio, A.; Rodriguez-Fortea, A.; Gervasio, F. L.; Ceccarelli, M.; Parrinello, M. *J. Phys. Chem. B* **2005**, *109*, 6714−6721.
(23) Car, R.; Parrinello, M. *Phys. Rev. Lett.* **1985**, *55*, 2471−2474.
(24) Gervasio, F. L.; Boero, M.; Parrinello, M. *Angew. Chem., Int. Ed.* **2006**, *45*, 5606−5609.
(25) Boero, M.; Ikeda, T.; Ito, E.; Terakura, K. *J. Am. Chem. Soc.* **2006**, *128*, 16798−16807.
(26) Perrin, C. L.; Lollo, C. P.; Johnston. E. R. *J. Am. Chem. Soc.* **1984**, *106*, 2749−2753.
(27) Kamiya, K.; Boero, M.; Shiraishi, K.; Oshiyama, A. *J. Phys. Chem. B* **2006**, *110*, 4443−4450.

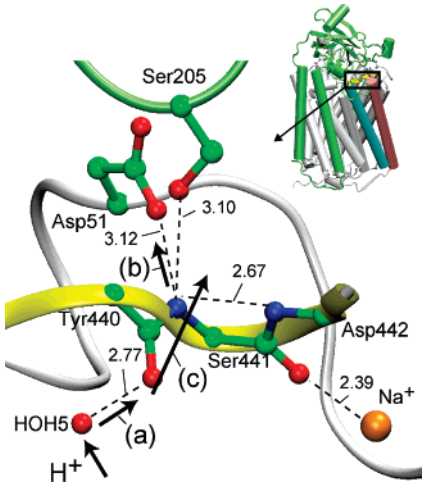

Figure 2. Schematic reaction for the proton transfer through the Tyr440-Ser441 peptide group in the bovine CcO. The labels a, b, and c indicate the processes studied in the present work. Here and in the following figures, the color code for atoms is green for C, red for O, blue for N, and orange for Na. A yellow ribbon indicates the C_α-trace of the Ω-like loop segment, while white and green tubes indicate the C_α-traces of the subunits I and II, respectively. (upper inset) The subunits I, the subunit II, the helices 22 and 23, and the helices 24 and 25 are shown in white, green, cyan, and pink, respectively. The numerical labels in the figure are the main distances expressed in Å.

peptide group (c in Figure 2), might be influenced by several structural features (Figure 2). The Tyr440−Ser441 peptide group is located in the Ω-like loop segment (from Gly435 to Tyr443) connecting the helices 22 and 23 (from Asn406 to Ser434) and the helices 24 and 25 (from Pro444 to Lys479). This segment is placed at the interface between the subunits I and II of the CcO and sandwiched between them. The Debye−Waller factors (B-factors), applied to the X-ray scattering term of each atom and indicating the degree of mobility, suggest a relatively high rigidity of this moiety. Interestingly, due to this turn conformation, the amide nitrogen of the adjacent Ser441-Asp442 peptide group points to that of the Tyr440-Ser441 peptide group. Furthermore, the carbonyl oxygen of the Ser441-Asp442 peptide group coordinates to the Na^+ metal cation. These features seem to indicate that the interplay among these elements could be an important catalytic factor for the promotion of the enol-to-keto tautomerization. In an attempt at covering all the possible pathways that a proton could follow in the transfer through the Tyr440-Ser441 peptide group, we investigated a series of three proton-transfer reactions (labeled as a, b, and c in Figure 2) occurring in this peculiar region, and elucidate the role of the local conformation of the enzyme.

On the basis of these calculations, we have identified a multistep proton-transfer mechanism that allows for the overcoming of the Tyr440-Ser441 peptide group in the bovine CcO, thus making possible the proton propagation along a network not entirely composed of H-bonds. Geometry optimizations indicate that the imidic acid of the Tyr440-Ser441 peptide group is formed as a metastable state, following a proton transfer to its carbonyl oxygen. Standard CP molecular dynamics simulations show that the deprotonated carboxyl group of the Asp51 side chain approaches this imidic acid and extracts the amide proton with a negligible activation barrier, converting the peptide group into the enol form. The surrounding serine residues (e.g., Ser205) can favor this reaction without undergoing large conformational changes. Subsequent metadynamics simulations reveal that the enol-to-keto tautomerization eventually occurs via a double proton transfer between the two adjacent Tyr440-Ser441 and Ser441-Asp442 peptide groups with a free-energy barrier of about 13 kcal/mol. The free-energy surface shows that the enol form is less stable than the keto form, providing further support to the unidirectional character of the proton-transfer reaction through a peptide group. The local rigid Ω-like loop conformation of the peptide backbone, along with the nearby Na^+ ion, brings the two peptide groups to face each other and is responsible for their different dynamical fluctuations, both favoring a double proton-transfer path. The present calculations clarify that the bovine CcO crystal structure around the Tyr440-Ser441 peptide group is particularly suited to promote a proton transfer through peptide groups.

2. Computational Details

The CcO model system used here (Figure 3) was constructed on the basis of the X-ray crystallographic data and mutagenesis experiments;[3,12] the relevant parts were extracted from the fully oxidized bovine CcO crystal structure.[3] The system was then placed in an orthorhombic simulation cell of sizes $a = 22.38$ Å, $b = 14.92$ Å, and $c = 20.67$ Å, thus being an isolated macromolecule separated from its periodically repeated images by a minimum distance of 6.5 Å. Our model consists of Tyr440, Ser441, Asp442, Asp51, His204, Ser205, HOH5, HOH69, and Na^+ with its ligands (Glu40, Leu41, Gly45, Thr46, and HOH26). In addition, an acetic acid and a 1-propen-2-ol are included to mimic the propionate A of heme *a* and the phenolic group of Tyr371 of subunit I, respectively. To reduce the computational costs, five amino acid residues, whose side chains are far from the active site, were replaced with Ala or Gly: Tyr440Ala, Asp442Ala, His204Ala, Leu41Gly, and Thr46Gly. As far as the protonation of the carboxyl groups is concerned, we had to rely on a comparison of the oxidized and reduced forms of the CcO as provided by the Protein Data Bank. In our model system, three carboxyl groups are present: Asp51, Glu40, and the propionate A of heme *a*. We did both an inspection of the local hydrogen-bond network and an analysis of the theoretical pK_a performed on a subsystem, including all the residues within a distance of 12 Å from the carbonyl O of the Tyr440-Ser441 peptide group via Poisson−Boltzmann solver, as provided by the PCE web service.[28] These analyses confirmed that a consistent choice is represented by a full protonation of both Glu40 and propionate A of heme *a*. As far as Asp51 is concerned, at pH = 7.0 the computed protonation turned out to be 0.79, a valuelower than 0.94 characterizing Glu40 and propionate A, yet shifted toward protonation. Nonetheless, as inferred from experiments,[3] the proton of Asp51-C_γOOH is expected to be the mobile one, coming from the peptide group and then released above it, as shown in Figure 1 and in ref 3. We then assumed Asp51 to be deprotonated, since in these conditions it can become a proton acceptor for the H^+ coming from the peptide group. All the peptide groups were assumed to be in a keto form, according to the experimental data; however, since a proton propagation process is the target of the present study, an additional H^+, corresponding to the uptake of a proton by the enzyme, was added to the crystal water HOH5. The resultant CcO model amounts to 120 atoms and 322 electrons and has a net charge $Q = +1$. Since a periodically repeated simulation cell was adopted, to avoid spurious interaction with neighbor images a uniform background charge $Q^{back} = -1$ was included to neutralize the system, according to the standard procedure adopted for charged systems on which periodic boundary conditions are applied.[29] The addition of one extra proton to the crystallographically identified O of HOH5 was driven by the

(28) Miteva, M. A.; Tufféry, P.; Villoutreix, B. O. *Nucleic Acid Res.* **2005**, *33*, W372−W375 (http://bioserv.rpbs.jussieu.fr/PCE). Since a maximum of 50 residues can be treated, we had to extract a subsystem from the whole CcO not exceeding this limit.
(29) Makov, G. and Payne, M. C. *Phys. Rev. B* **1995**, *51*, 4014−4022.

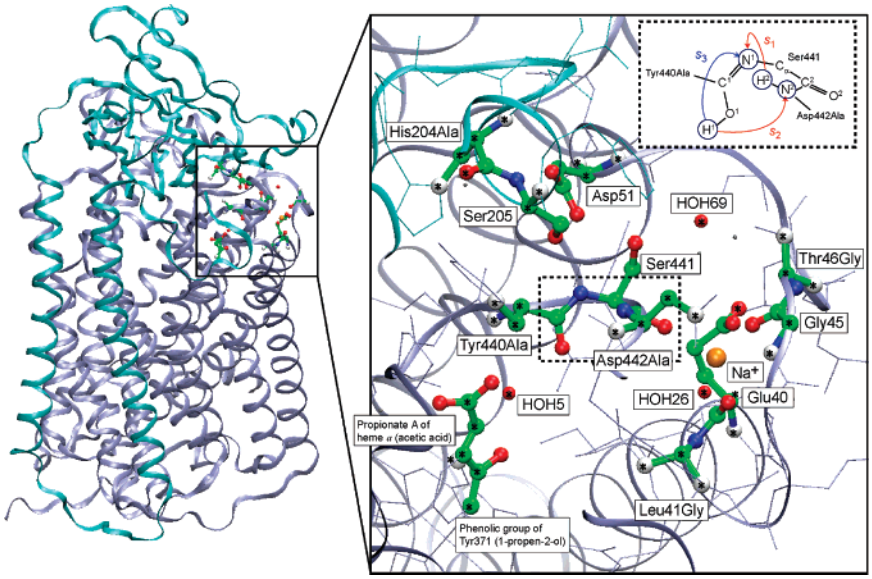

Figure 3. Figure 3. The CcO model system used in this work (right panel) and its position inside the bovine CcO (left panel); only subunit I and subunit II are shown for the sake of clarity. The atoms composing the model system are shown as balls and sticks with the same color code of the previous figure. Subunits I and II are evidenced in gray and cyan, respectively. The restrained capping H atoms are shown as white balls. All the atoms subject to constraints (see text) during the simulations are marked by an asterisk. The upper right inset shows all the collective variables used in the present study.

Scheme 2

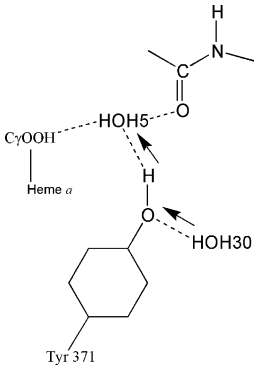

suggestion of ref 12. In fact, by looking at Figures 1 and 2 of that experimental work and the Protein Data Bank related file, it is clear that the O atom of HOH5 is the only possible donor hydrogen bonded to the −C═O group of Tyr440. Provided that the H-path is active, a proton traveling along this pathway can then arrive to the Tyr440-Ser441 peptide group upon a protonation−deprotonation process of this HOH5 that, by accepting an incoming H^+ and reverting to hydronium OH_3^+, donates the excess proton to this −C═O group of Tyr440 that, in turn, reverts to −C−O−H. Hydronium is known to be very acidic at 300 K, with a pK_a of −1.7 in solution. However no detailed information has been reported to date for the bovine CcO and related redox chemistry. Instead, the protonation of HOH5 water is discussed on the basis of structural data in ref 10 and sketched in Scheme 2, where the arrows indicate the path followed by a proton during its trip along this particular segment of the H-path.

Basically, the crystal water HOH30 is expected to receive the incoming proton and becoming an OH_3^+, then donate it to the phenolic group of Tyr371 that, in turn, can donate a H^+ to HOH5. This is the configuration that we assumed as the initial step in the whole peptide group reaction discussed in the next paragraphs. The model system adopted here has indeed all the features and local hydrogen-bond network structure needed to correctly reproduce the environment around the active peptide group; simulations conducted on a smaller model in which 101 atoms were included and side chains relevant to propionate A of heme *a* and the phenolic group of Tyr371 were omitted gave chemically inconsistent reaction paths and related free-energy profiles, underscoring that excessive removal of side chains would result in unreliable systems. Furthermore, the reaction pathway obtained on this small model showed permanent large deviations from the crystallographic data both during the reaction and in the final structure.

No information is available concerning the exact position of lipid bilayers surrounding the CcO, and their influence on the global H-path is still unknown. However, the bilayers are very far from the catalytic site considered here. Namely, the minimum distance between the peptide group undergoing the reaction and helix 69, the closest external helix facing the lipid bilayer, is about 26 Å. Bilayers are then located at least beyond this distance, thus having in practice no influence on the active site, which is well screened by the surrounding helices constituting the CcO, at least for this peculiar reaction involving the tautomerization of an inner peptide group.

Geometry optimizations were performed on the present CcO system within our density-functional approach, to eliminate any residual bond stress that could possibly bias the simulated reactions. To this aim, we used a standard conjugated gradient procedure until the residual forces were lower than 0.6 kcal/mol/Å. During the geometry optimization, the positions of several atoms at the boundaries (asterisked in Figure 3) were fixed to their X-ray crystallographic positions to emulate the constraining effects of the protein environment. In the subsequent dynamical simulations, these atoms were allowed to oscillate around these positions by bounding harmonic potentials whose force constants were set to be 6.5 or 26.0 kcal/mol/Å.[2] In addition, the Ψ torsion angle of Tyr440Ala was constrained to the corresponding crystal structure value by a harmonic force constant of 0.019 kcal/mol/degree,[2] to account for the effect of the surrounding amino acid residue (Tyr54).

All first-principles molecular dynamics simulations[30] were performed assuming as a starting configuration the optimized CcO model. We work in the framework of the DFT-based Car−Parrinello scheme, with gradient corrections on the exchange and correlation functional after Hamprecht, Cohen, Tozer, and Handy (HCTH).[31] Valence-core electron interactions are described by Troullier−Martins norm-conserving pseudopotentials;[32] in the case of Na, semicore states, 2s and 2p, are included. Valence electrons are represented in a plane wave basis set

(30) CPMD, Copyright IBM Corp., 1990−2006; Copyright MPI für Festkörperforschung Stuttgart, 1997−2001.
(31) Hamprecht, F. A.; Cohen, A. J.; Tozer, D. J.; Handy, N. C. *J. Chem. Phys.* **1998**, *109*, 6264−6271.
(32) Troullier, N.; Martins, J. L. *Phys. Rev. B* **1991**, *43*, 1993−2006.

with an energy cutoff of 80 Ry. The ionic temperature is controlled by velocity rescaling and kept at 300 ± 40 K. An integration time step of 0.097 fs and a fictitious electron mass of 400 au ensure a good control of the conserved quantities and preserve the Born−Oppenheimer adiabaticity.[33,34]

The reaction paths were sampled by the metadynamics approach;[21,22] the collective variables $s_\alpha(t)$ ($\alpha = 1, 2, ...$) selected as representative of the reaction coordinates are treated as new dynamical variables and added to the CP Lagrangian L^{CP} along with a history-dependent Gaussian potential $V(s_\alpha, t)$ as described in ref 21,that is,

$$L = L^{CP} + \frac{1}{2}\sum_\alpha M_\alpha \dot{s}_\alpha^{\,2} - \frac{1}{2}\sum_\alpha k_\alpha [s_\alpha(q) - s_\alpha]^2 + V(s_\alpha,t) \quad (1)$$

where $s_\alpha(q)$ can be any function of an arbitrary set of ionic coordinates, $q = \{\mathbf{R}_{ion}\}$, suitable to describe the process that we want to simulate, and M_α and k_α are fictitious effective masses and harmonic coupling constants, both of them being used for the adiabatic decoupling between fast and slow degrees of freedom. In our specific case, we selected as s_α three distances: N^1-H^2 (s_1), N^2-H^1 (s_2), and N^1-H^1 (s_3) (see inset in Figure 3). These variables represent all the slowly varying degrees of freedom and account for the formation and cleavage of each N−H bond occurring during the proton transfer. Two types of reaction paths were investigated: a double-step and single-step proton transfer. In the first case, two variables, s_1 and s_2, were used, whereas only s_3 was used in the second case. In all simulations $M_1 = M_2 = M_3 = 12.0$ au and $k_1 = k_2 = k_3 = 0.24$ were adopted. A new Gaussian penalty potential was added every 4.85 fs and its width and height are sampled in the intervals [0.132, 0.265] Å and [0.7, 2.5] kcal/mol, respectively. To obtain a homogeneous dynamics for all the s_α variables, the width of the Gaussians for s_2 was scaled by a factor two. A confining potential (V_{conf}) was introduced to limit the sampling of s_1 or s_3 to phase space corresponding to the enol-to-keto tautomerization and to prevent local conformational changes incompatible with the CcO crystal structure. This additional potential has the analytical form $V_{conf} = 31.4\,(s_\alpha/0.79)^4$ kcal/mol and becomes effective whenever $s_\alpha > 3.97$ Å.

3. Results and Discussion

3.1. Formation of Enol Form of the Tyr440Ala-Ser441 Peptide Group via Imidic Acid. In the mechanism proposed for the H-pathway,[3,7,10,11] the protonated carboxyl group of the Asp51 side chain ($C_\gamma OOH$) releases its proton. Once that it is deprotonated, it moves back toward the interior of the protein upon heme *a* oxidation, and at this point it becomes a proton acceptor. The next H^+ reaches, via a proton wire mechanism,[8,9] the crystal water molecule HOH5 located at a H-bond distance from the carbonyl O of the Tyr440-Ser441 peptide group, transforming the water molecule into hydronium H_3O^+.

The geometry optimizations performed on the CcO model system in this situation, that is, the deprotonated carboxyl group of the Asp51 side chain ($-C_\gamma OO^-$) and protonated water (H_3O^+), have shown that the additional proton in the H_3O^+ transfers spontaneously to the carbonyl oxygen of the keto form of the Tyr440Ala-Ser441 peptide group, leading to the formation of the imidic acid. This is not surprising, because the H_3O^+ is initially in a destabilized Eigen complex configuration, and it has been already shown that such destabilized complexes behave like an acid.[19,35] On the other hand, the carboxyl group of Asp51 remains deprotonated after the system is fully relaxed. These results indicate that the imidic acid of the Tyr440Ala-Ser441 peptide group can be regarded just as a metastable state in the bovine CcO environment.

The subsequent step is the reaction leading to the formation of the enol form of the Tyr440Ala-Ser441 peptide group. To investigate this step, we performed ordinary unconstrained CP molecular dynamics simulations at room temperature ($T = 300$ K) starting from the relaxed configuration discussed in the previous paragraph. Upon dynamics, the present CcO system shows that the reaction occurs in an almost barrierless way: simple thermal fluctuations turn out to be enough to activate and promote the process. These results are summarized in Figure 4. Namely, the deprotonated carboxyl group of the Asp51 side chain approaches the imidic acid of the Tyr440Ala-Ser441 peptide group (Figure 4a) and extracts the amide proton dislodged along the H-bond with a negligible activation barrier (Figure 4b), converting the Tyr440Ala-Ser441 peptide group into the enol form (Figure 4c). Subsequently, within a simulation time of about 1 ps, this same proton undergoing the transfer returns back from the carboxyl group of Asp51 to the Tyr440Ala-Ser441 peptide group, leading to the re-formation of the imidic acid (Figure 4d and e). This situation indicates that the system is in a sort of bistable configuration with two shallow minima, imidic acid and enol form, separated by an activation barrier of the order of k_BT.

When the proton transfer occurs (Figure 4b and d), the surrounding amino acid residues, especially Ser205, form H-bonds with the O atom of the carboxyl group of the Asp51 side chain ($O_\delta{}^1$ in Figure 4), leading to a decrease of the distance between proton donor and acceptor. At the same time, these residues set the directions of the donor and acceptor sites in such a way that the plane defined by the $C_\gamma OO$ group of Asp51 is almost perpendicular to the Tyr440Ala-Ser441 peptide plane. This double action leads to a strengthening of the H-bond between the Tyr440Ala-Ser441 peptide group and the Asp51 side chain ($N-H-O_\delta{}^2$ in Figure 4). Indeed, the resultant H-bond lengths and angles are 2.43/2.45 Å and 166°/152°, respectively, in the configurations labeled as b/d in Figure 4, promoting the proton transfer. As inferred from studies of simple model systems,[16,36] the energy barrier for proton transfer via H-bond depends on both the radial and angular deformations of the H-bond involved.

3.2. Enol-to-Keto Tautomerization of the Tyr440Ala-Ser441 Peptide Group. Contrary to the two steps discussed above, the enol-to-keto tautomerization of the Tyr440Ala-Ser441 peptide group is not expected to occur spontaneously. In fact, this process is supposed to be the rate-limiting step characterized by an energy barrier that simple thermodynamic fluctuations are unable to overcome. Hence, we sampled the reaction path by using the metadynamics approach to inspect the tautomerization mechanism. We started this simulation from the same ionic configuration and velocities obtained at the end of the previous CP molecular dynamics. This corresponds to the conformation shown in Figure 4e and represents a well-equilibrated situation in which all the fast events that can occur upon temperature effects already occurred and the system is in a stable local minimum. In this particular configuration, the Tyr440Ala-Ser441 peptide group assumes the imidic acid form,

(33) Grossman, J. C.; Schwegeler, E.; Draeger, E. W.; Gygi, F.; Galli, G. *J. Chem. Phys.* **2004**, *120*, 300−311.
(34) Schwegeler, E.; Grossman, J. C.; Gygi, F.; Galli, G. *J. Chem. Phys.* **2004**, *121*, 5400−5409.
(35) Boero, M.; Ikeshoji, T.; Terakura, K. *ChemPhysChem* **2005**, *6*, 1775−1779.
(36) Scheiner, S. *J. Am. Chem. Soc.* **1981**, *103*, 315−320.

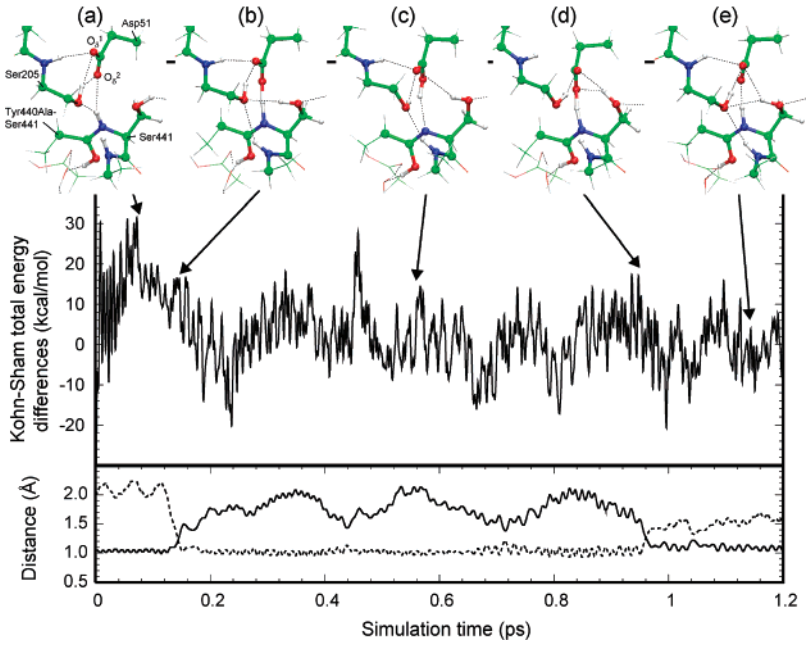

Figure 4. Total energy as a function of the simulation time relative to the reaction leading to the enol form at 300 K. The snapshots shown above the energy plot and labeled from a to e represent the main steps of the reaction; the principal atoms are shown as balls and sticks. The H-bonds are indicated by dotted lines. The plot in the lower panel refers to the evolution of the distances between the departing H and the amide N of the Tyr440Ala-Ser441 peptide group (solid line) or the carboxyl O (O_δ^2) of the Asp51 side chain (dashed line).

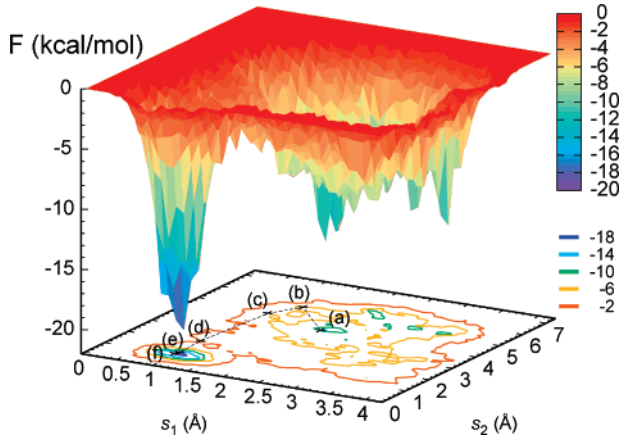

Figure 5. Reconstructed free-energy landscape in the space defined by the collective variables for the enol-to-keto tautomerization. The collective variable indicated as s_1 is the N^1-H^2 distance, while s_2 is the N^2-H^1 distance. The labels a−f refer to the configurations shown in Figure 6.

whereas the carboxyl group of the Asp51 side chain is in the deprotonated form. The collective variables were chosen to be two N−H distances in the two adjacent Tyr440Ala-Ser441 and Ser441-Asp442Ala peptide groups, labeled as s_1 (N^1-H^2) and s_2 (N^2-H^1) in the inset of Figure 3. These variables account for the transfers of the two protons, and their simultaneous action allows for a direct check of the energetic order of these two transfers. The results are summarized in Figures 5 and 6 as far as the free-energy profile and the main stages of the reaction are concerned.

In the early stage of the metadynamics simulation (within 0.2 ps), the amide proton of the imidic acid is rapidly transferred to the carboxyl oxygen of the Asp51 side chain because a H-bond between the amide N and the carboxyl O is still present. This leads to the formation of the enol form of the Tyr440Ala-Ser441 peptide group. During the following 7.5 ps, the system explores a large basin of the free-energy landscape (Figure 5), keeping the peptide group in the enol form. The representative configuration corresponding to this local minimum (labeled as a in Figure 5) is shown in Figure 6a. In terms of collective variables evolution (Figure 7a), this exploration is represented by the values of s_1 ranging from 1.2 to 3.8 Å, with s_2 values confined into the interval [1.2, 6.2] Å.

An inspection of the reactive trajectory shows that at about 4.2 ps the system makes a first attempt toward the transition, marked by a jump of s_1, meaning that it is trying to transfer the proton to the amide N of the enol form. During this transient process, the H-bond between this amide N and the carboxyl O of Asp51 is broken, and the carboxyl group of Asp51 departs from the enol form and forms H-bonds with the surrounding Ser205 and Ser441 residues.

When the system escapes from this wide basin, it undergoes the first proton-transfer reaction in which the proton of the Ser441-Asp442Ala peptide group is transferred to the amide nitrogen of the Tyr440Ala-Ser441 one (Figures 5a−c and 6a−c), via a five-membered ring structure of the atoms involved in this process (Figure 6b). This is evidenced in the collective variables evolution (Figure 7a) as a jump of s_1 at 7.5 ps, while s_2 remains practically unaffected. After this first proton transfer, the system immediately undergoes the second one, overcoming a small free-energy barrier of about 5 kcal/mol, indicating that this double proton jump is almost concerted. In this case, the proton of the carbonyl oxygen of the Tyr440Ala-Ser441 peptide group transfers to the amide nitrogen of the Ser441-Asp442Ala one (Figures 5c−f and 6c−f), via the formation of a seven-membered ring structure (Figure 6e). Eventually the system finds a stable local minimum in which both the Tyr440Ala-Ser441 and the Ser441-Asp442Ala peptide groups are in the keto form (Figure 6f). By looking at the reconstructed free-energy profile (Figure 5), the final product (labeled as f in Figure 5; $s_1 = 1.08$ Å, $s_2 = 1.02$ Å) is more stable than the reactant (labeled as a in Figure 5; $s_1 = 2.04$ Å, $s_2 = 4.17$ Å), and this is consistent

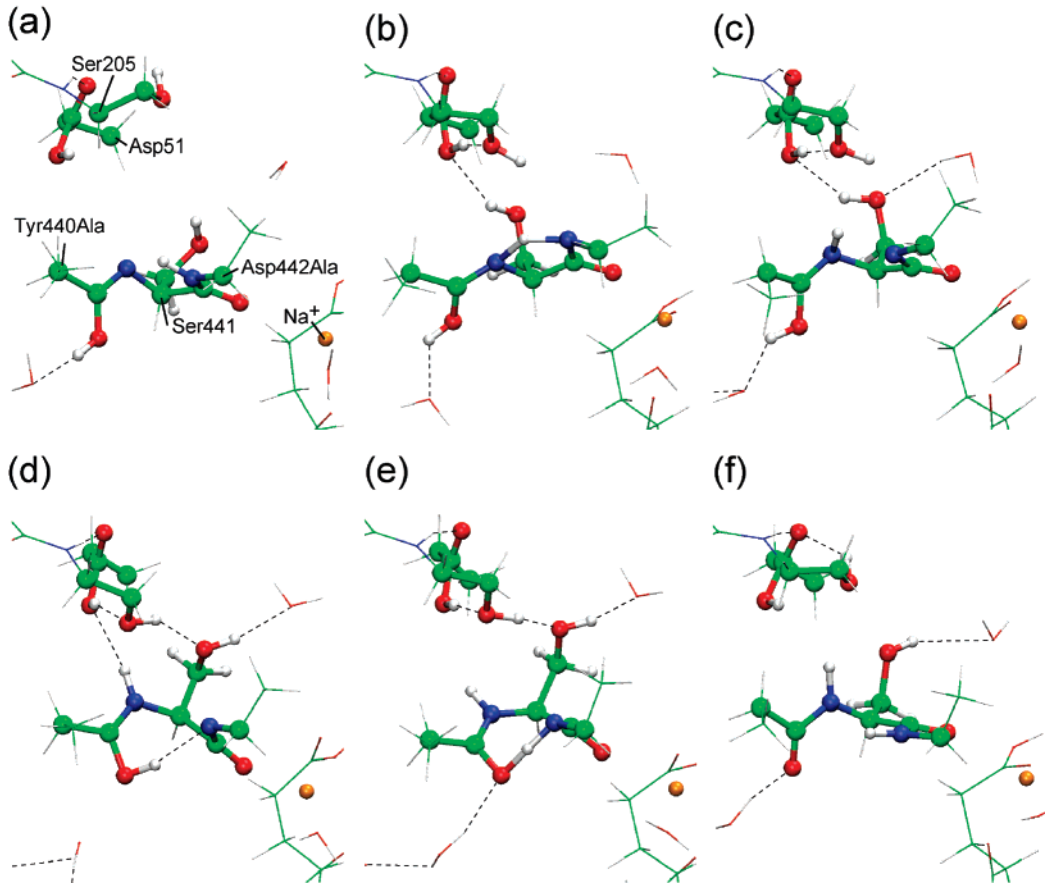

Figure 6. Snapshots of the structures of the various intermediate states realized by the system during the enol-to-keto tautomerization. The labels a−f refer to the position on the free-energy surface shown in Figure 5. The most relevant atoms are drawn as balls and sticks, and hydrogen bonds are indicated by dashed lines.

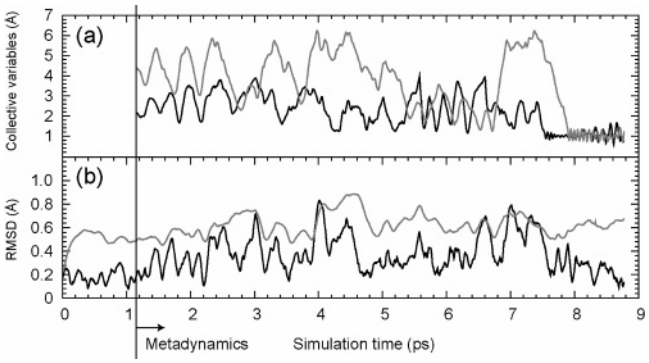

Figure 7. Evolution of (a) the collective variables and (b) the rmsd during the simulation: the vertical line separates the standard molecular dynamics (on the left with respect to this line) from the subsequent metadynamics (on the right with respect to this line). (a) The two collective variables s_1 and s_2 are shown as black and gray lines, respectively. (b) The rmsd values were measured for the backbone heavy atoms of the Tyr440Ala-Ser441-Asp442Ala segment (black line) and for all the heavy atoms present in our model system (gray line).

with both experimental[26] and theoretical[27] results that the keto is the stable conformation in model peptide systems. Furthermore this provides support to the unidirectional character of the proton-transfer reactions through the Tyr440-Ser441 peptide group. The overall free-energy barrier,[37] estimated in terms of difference between reactant (a) and transition state (labeled as d in Figure 5; $s_1 = 0.99$ Å, $s_2 = 2.15$ Å), is about 13 kcal/mol.

It must be remarked that during the whole process, the movement of the atoms not belonging to the peptide group undergoing the chemical reaction is always rather modest. The major displacement observed is the one of Ser205 from the initial configuration (Figure 6a) to the transient structure of Figure 6d; by considering the heavy atoms C_α, C_β, and O_γ of Ser205, identified by their Cartesian positions $\mathbf{R}^{\mathrm{Ser205}}(\mathrm{a})$ in the initial configuration and $\mathbf{R}^{\mathrm{Ser205}}(\mathrm{d})$ in the transient maximally displaced state, we obtained $\Delta\mathbf{R}^{\mathrm{Ser205}} = \sqrt{\langle \mathrm{R}^{\mathrm{Ser205}}(\mathrm{d}) - \mathrm{R}^{\mathrm{Ser205}}(\mathrm{a})\rangle^2} = 1.7$ Å, a value that is however lower than the X-ray resolution of 1.8 Å for this system[3] and thus still compatible with the experimental outcome. In any case, this configuration is realized just as a transition structure during the phase space sampling, and this displacement does not represent a permanent conformational change of the system, which in the final (stable) state is indeed close to the crystallographic. In fact, the root-mean-square deviation (rmsd) from the bovine CcO crystal structure shows that the system reaches a final state having a conformation very close to that of the original crystal structure. Panel b of Figure 7 shows the rmsd evolution during the present simulations for the backbone heavy atoms (C_α, C, O, and N) in the segment from Tyr440Ala to Asp442Ala (black line) and for all heavy atoms in the calculation model (gray line). As can be seen, the present metadynamics simulation starts with a configuration close to the X-ray structure and preserves it in the final state, reflecting the relative rigidity of this loop segment and showing that no permanent conformational changes are induced by the double proton-transfer

(37) Kollman, P. *Chem. Rev.* **1993**, *93*, 2395−2417.
(38) Takano, Y.; Nakamura, H. *Chem. Phys. Lett.* **2006**, *430*, 149−155.

process. The flexibility of the backbone conformation in the vicinity of the peptide group has been shown to lead to an enol-to-keto tautomerization in polyglycine,[27] where the energetically most favorable reaction path is realized by a cis−trans isomerization of the C−N peptide bond. In the case of CcO, the experimental data seem to suggest that the segment containing the Tyr440-Ser441 peptide group is instead rather rigid, as discussed in the introduction, thus making a cis−trans isomerization more problematic. In polyglycine, however, we saw that a direct proton transfer from O to N can be realized. To verify whether or not a similar direct H^+ transfer represents a viable possibility also in CcO, we performed an auxiliary metadynamics simulation by using as a single collective variable the N^1-H^1 (s_3 in the inset of Figure 3) in the Tyr440Ala-Ser441 peptide group. This accounts for a direct proton transfer not involving other groups. As expected from our previous studies[27] and recent Hartree−Fock calculation,[37] the transition state takes a distorted four-member ring structure of atoms belonging to this Tyr440Ala-Ser441 peptide group. Such large deformations and bond stresses necessary to achieve the proton transfer have the effect of increasing the free-energy barrier of the process of more than a factor of two with respect to the case of the double proton transfer. This clearly indicates that a single step mechanism is not the preferred pathway to the enol-to-keto tautomerization, although also in this case no permanent conformational changes are induced.

3.3. Geometrical and Electronic Structure Analyses. In the case of the enol formation, the deprotonated carboxyl group of the Asp51 side chain approaches the amide proton of the imidic acid when the proton transfer occurs, assisted by Ser205 (Figure 4b). This is consistent with the bovine CcO crystal structure (Figure 8a) in the sense that Asp51 and Ser205 are positioned in the α helix (residues 50−68 of subunit I) and in the 3_{10} helix (residues 203−207 of subunit II), respectively, and their side chains both point to the Tyr440-Ser441 peptide group. The experimental B-factors indicate that the carboxyl group of Asp51 is highly flexible, whereas the Ser205 side chain and the Tyr440-Ser441 peptide group are both relatively rigid. Coming to the enol-to-keto tautomerization, by superimposing the related snapshots onto the corresponding parts of the X-ray structure (Figure 8b and c), we remark that when the proton transfers take place the Tyr440Ala-Ser441 peptide group undergoes a significant displacement, while the adjacent Ser441-Asp442Ala peptide group is basically unaffected.

More precisely, a close inspection of the backbone torsion angles Φ and Ψ (Figure 8b and c), which define a tilt between two neighboring peptide planes with the C_α of Ser441 at the center of rotation, shows that the Φ values are characterized by large fluctuations, whereas Ψ ones do not depart significantly from the experimental value ($\Phi = -84°$ and $\Psi = -14°$ in the crystal). These fluctuations, however, occur only during the reaction and do not affect the final product that, indeed, is close to the X-ray crystal structure. Yet, they are compatible with the fact that in the bovine CcO these two peptide groups face each other and the carbonyl oxygen of Ser441 coordinates with the Na^+ cation. In these conditions the N−H direction of the Ser441-Asp442Ala peptide group points toward the Tyr440Ala-Ser441 one, without requiring large changes in the Ψ torsion angle. Instead, a change of Φ is necessary (and sufficient) to shorten the proton donor−acceptor distances, thus promoting the double proton transfer.

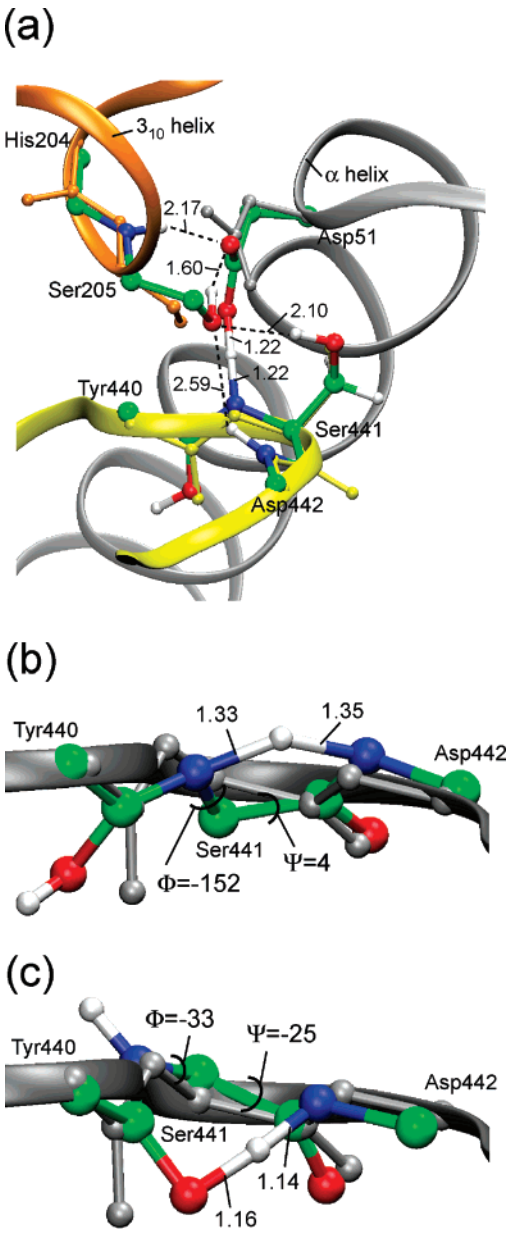

Figure 8. Geometrical structures representing the transition states relative to (a) the reaction yielding the enol form and (b and c) the enol-to-keto tautomerization. The most relevant atoms are shown by balls and sticks for the sake of clarity. The snapshots are superimposed to the corresponding X-ray derived coordinates of the bovine CcO crystal structure; the X-ray experimental positions are colored in yellow, orange, and black, according to whether they belong to subunit I (gray), subunit II (orange), or Ω turn (yellow). Distances and angles are expressed in Å and degrees, respectively.

When the proton transfer occurs, the related Kohn−Sham (KS) electron states show that valence electrons are delocalized over the donor-H^+-acceptor moiety (Figure 9), and this seems to contribute to the stabilization of the transient structures the system goes through. In the case of the enol formation the proton transfer occurs in such a way that the deprotonated carboxyl group of the Asp51 side chain, that is, -$C_\gamma OO$, approaches to the Tyr440Ala-Ser441 peptide group. In these conditions the planes formed by $C_\gamma OO$ and the peptide group are almost perpendicular to each other, and the departing proton belongs to both the planes (Figure 8a). This peculiar configuration brings

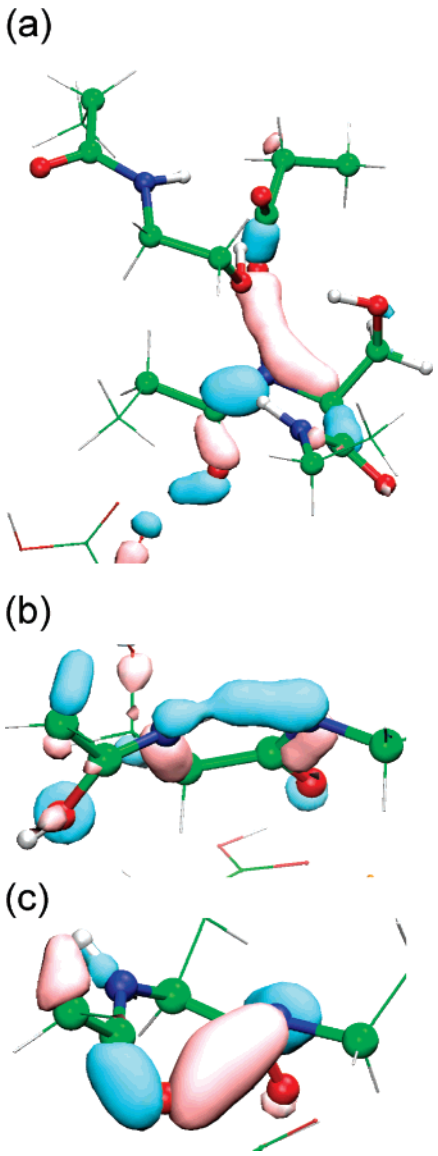

Figure 9. Some representative occupied KS states relative to (a) the enol formation and (b and c) the enol-to-keto tautomerization. The underlying geometries are the same reported in Figure 8. Each KS orbital corresponds to (a) the 105th state below the highest occupied KS (HOKS) orbital (HOKS-105), (b) the 88th state (HOKS-88), and (c) the 105th state (HOKS-105). All isosurfaces are at +0.19 (pink) and −0.19 (light blue) $(e/Å^3)^{1/2}$.

to an alignment of the 2p orbitals of the proton donor (N) and acceptor (O) atoms, and as a consequence these orbitals hybridize with the 1s state of H, leading to the formation of the electron state delocalized over the N−H−O moiety (Figure 9a). As a further quantitative check, we performed a Mulliken population analysis on this configuration, finding that this transferred H is characterized by a charge of +0.285, much smaller than the value for a bare proton. This indicates that the nature of this departing H is closer to a hydrogen rather than a bare proton until the N−H chemical bond is not completely cleaved and is in agreement with the *double well* nature of general proton transfers, for which the transition state theory does not hold.[39]

As mentioned, the double proton transfer in the enol-to-keto tautomerization passes across the formation of five- and seven-membered ring structures (Figure 8b and c). In both cases the Tyr440Ala-Ser441 peptide plane tilts toward the Ser441-Asp442Ala peptide plane, due to the rigidity of their backbone conformation, leading to a configuration in which the departing H is out of these planes. Nonetheless the KS states (Figure 9b and c) show again that the 2p orbitals of the donor and acceptor atoms are hybridized with the H 1s atomic orbital, contributing to a bonding-like KS state delocalized around the donor-H^+-acceptor moiety. As expected, these KS states contribute to the increase in the electron distribution around the transferring H, and this picture is quantitatively supported by the Mulliken population analysis (H^2 in the state b and H^1 in the state e in Table 1).

Table 1. Mulliken Atomic Charges of the Main Atoms and Peptide Groups of the Intermediate States in the Enol-to-Keto Tautomerization[a]

state	O^2	Na^+	H^2	H^1	Tyr440Ala-Ser441	Ser441-Asp442Ala
a	−0.347	+0.944	+0.320	+0.356	−0.162	−0.202
b	−0.394	+0.927	+0.215	+0.435	−0.198	−0.292
c	−0.384	+0.926	+0.304	+0.360	−0.074	−0.367
d	−0.424	+0.957	+0.338	+0.360	−0.027	−0.378
e	−0.336	+0.928	+0.356	+0.314	−0.121	−0.278
f	−0.324	+0.939	+0.294	+0.318	−0.137	−0.197

[a] Atom labels correspond to the ones given in Figure 3, while labels from a to f refer to the states indicated in Figures 5 and 6. The atomic charges of each state are averaged over all the energetically close configurations. The Mulliken charge of each peptide group is simply the sum over all the constituent N, C, and O atoms.

The role of the Na^+ metal cation located in proximity of the carbonyl O of the Ser441-Asp442 peptide group (Figure 2) has not yet been clarified.[7] From the present calculations we can infer that the Na^+ ion plays at least two roles in the double proton-transfer mechanism. First, the Na^+ ion helps in fixing the Ser441-Asp442Ala peptide group orientation in such a way that its N−H bond points toward the amide N of the Tyr440Ala-Ser441 group, thus favoring the proton transfer. Second, this cation contributes to the stabilization of the intermediate states in which the Ser441-Asp442Ala peptide group assumes the imidate-anion form (Figure 6c and d). In terms of Mulliken population analysis (Table 1) the charges of the atoms of the Ser441-Asp442Ala peptide group become more negative in these intermediate states (Table 1, c and d), in comparison with the other states. During the lifetime of these states (7.5 to ∼7.9 ps) the distance between the carbonyl O of the Ser441-Asp442Ala peptide group and Na^+ cation decreases to its minimum (∼2.0 Å) and keeps a small value, around 2.3 Å, until the second proton transfer occurs, suggesting a contribution to the stabilization of these intermediate states via a $Na^+-O^{\delta-}$ Coulomb interaction. Interestingly, in the bacterial CcO, the corresponding metal cation (Ca^{2+}) is located far from the Ile476-Asp477 peptide group, which corresponds to the Ser441-Asp442 one in the bovine CcO, because of an insertion of an amino acid residue (Glu63 in the bacterial CcO) in the ligand backbone segment.[40] Thus, this cation is not able to coordinate to the carbonyl O of the peptide group, suggesting that in the bacterial CcO the neighboring Ile476-Asp477 peptide group might not be used for the proton transfer through the Tyr475-Ile476 peptide group corresponding to the Tyr440-Ser441 one in the bovine CcO.

(39) Marx, D.; Tuckerman, M. E.; Hutter, J.; Parrinello, M. *Nature* **1999**, *397*, 601−604.

(40) Abramson, J.; Svensson-Ek, M.; Byrne, B.; Iwata, S. *Biochim. Biophys. Acta* **2001**, *1544*, 1−9.

Scheme 3

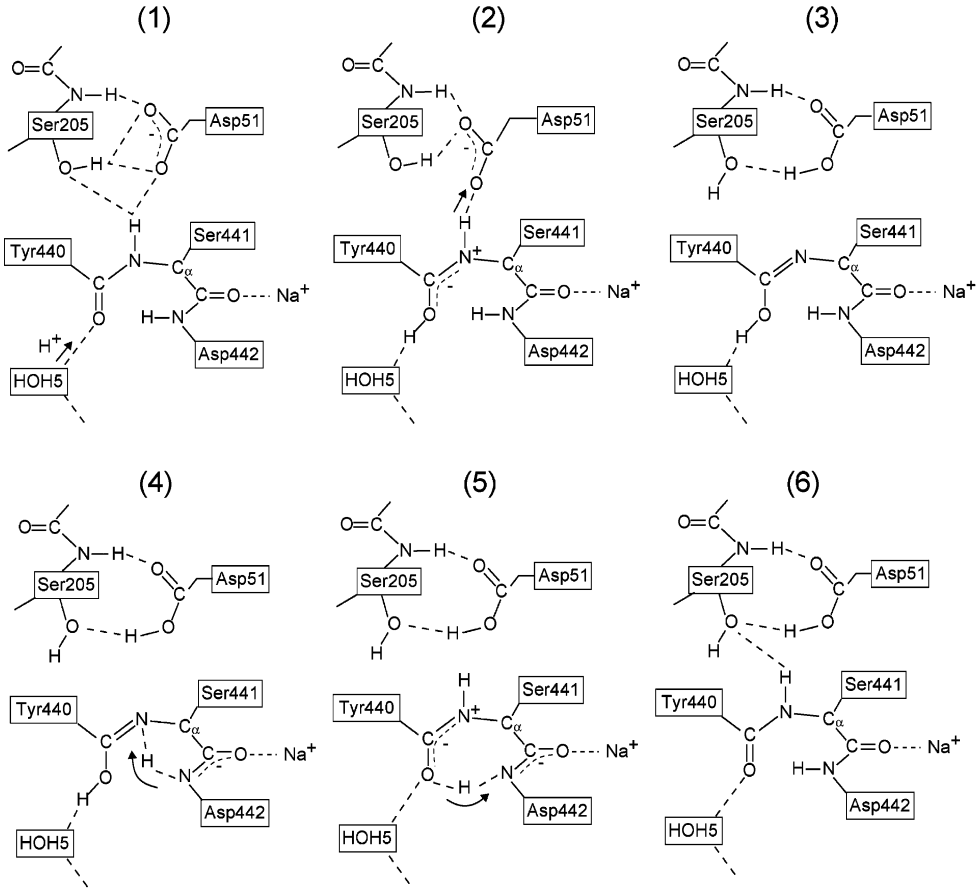

As inferred from several resonance Raman and infrared spectroscopy studies, the heme *a* has been suggested to be a driving element in the proton transfer through the H-pathway.[3,10,11] The propionate and formyl groups of the heme *a* form H-bonds with the Arg38 side chain and the crystal water HOH5, respectively, in the bovine CcO crystal structure. Thus, the H-path passes close to the heme *a*, instead of the O_2 reduction site. In this case proton transfers could induce changes of the electronic structures of both the formyl and propionate groups, influencing, in turn, those H-bonds formed with the Arg38 side chain and HOH5.[3,10,11] Similarly, such changes might further affect the H-bond between HOH5 and the carbonyl O of the Tyr440-Ser441 peptide group, suggesting that the redox of heme *a* could influence the whole proton-transfer mechanism depicted in the present study, although this issue still awaits for an experimental confirmation. In this respect, the present multistep proton-transfer mechanism can provide a basis for forthcoming studies. Further detailed investigations within a hybrid QM/MM approach are required to elucidate interaction mechanisms between heme *a* and the residues and side chains directly or indirectly involved in the H-path. This is particularly true for the Tyr54 side chain, that is rather close to the Tyr440-Ser441 peptide group (about 3.6 Å for the shorter Tyr440-Tyr54 distance in the crystal structure) and could have some influence in the local bonds flexibility. Since this interaction is purely van der Waals, it cannot be described by present full quantum approaches.

4. Conclusions

On the basis of the density functional theory-based molecular dynamics calculations presented here, we propose a multistep proton-transfer mechanism for the H pathway of the bovine cytochrome *c* oxidase, where the rate-limiting step is the crossing of a peptide group. This particular step, involving the breaking and the formation of chemical bonds, represents the peculiarity of the H-path in CcO with respect to the most common D-path and K-path, which involve only the propagation of protons across a regular H-bond network. In this respect these two paths can well be rationalized in terms of the Grotthuss mechanism for proton wires, thus involving only rather modest activation barriers. On the contrary, the crossing of a peptide group is energetically more demanding and could hinder the proton propagation.

According to the mechanism studied here, this seems not to be the case: a proton can be transferred through the Tyr440-Ser441 peptide group, although in a way deeply different from a conventional proton wire. The proposed mechanism does not affect permanently the experimental crystal structure and can be realized by a set of well assessed chemical reactions (Scheme 3). In the first step, the HOH5 crystal water is expected to accept the incoming proton and become a transient hydronium, then, upon a Grotthuss propagation process, the protonated HOH5 donates the excess proton to the carbonyl oxygen of the Tyr440-Ser441 peptide group (Scheme 3, structure 1), leading to the formation of an imidic acid as a metastable state. The amide proton then transfers spontaneously at room temperature via a

Grotthuss-like mechanism (Scheme 3, structure 2), producing an enol form of the Tyr440-Ser441 peptide group (Scheme 3, structure 3). Structural and electronic modifications seem to promote this process. Namely the deprotonated carboxyl group of the Asp51 side chain approaches the imidic acid, assisted by Ser205, in such a way that a strong hydrogen bond between the carboxyl O and the amide N is formed; at the same time electrons are delocalized over the donor-H^+-acceptor moiety.

A subsequent enol-to-keto tautomerization occurs via a double proton-transfer path, consisting of the transfer of a H^+ from the amide N of the Ser441-Asp442 peptide group to the amide N of the Tyr440-Ser441 one (Scheme 3, structure 4), followed by another H^+ transfer from the carbonyl O of the Tyr440-Ser441 peptide group to the amide N of the Ser441-Asp442 one (Scheme 3, structure 5), reverting both these peptide groups into a keto form (Scheme 3, structure 6). The relative rigidity of the Ω-like loop backbone configuration and the nearby Na^+ ion both can favor this series of transfer reactions. The enol-to-keto tautomerization turns out to be the rate-limiting step of the whole reaction, characterized by a free-energy barrier of about 13 kcal/mol, whereas the former steps occur spontaneously at room temperature, evidencing a rather modest activation energy of the order of k_BT. In this tautomerization the product is characterized by a higher stability with respect to the reactant, supporting the notion of the unidirectionality of this particular proton pumping activity. As a word of warning, we remark that the absolute values of the activation energies estimated here may be biased by several factors, such as deficiencies in the model adopted, in the level of the theory, in the selected reaction coordinates, etc. Yet, the general reaction scheme and the qualitative picture that they provide, supported by the comparison to the X-ray structure in the various stages, can shed light into this novel proton-transfer process and complement the information not directly accessible to experiments.

Acknowledgment. We grateful acknowledge fruitful discussions with M. Iannuzzi, A. Laio, and F. L. Gervasio. This work is partly supported by grants-in-aid from MEXT under contract Nos. 17064002, 18036003, and 18054004. Computations were performed on the computer facilities at Academic Computing and Communications Center, University of Tsukuba, at Institute for Solid-State Physics, University of Tokyo, at Research Center for Computational Science, Okazaki Research Facilities, National Institutes of Natural Sciences, and at the Computer Center for Agriculture, Forestry, and Fisheries Research, MAFF, Japan.

JA070464Y